J. Biochem. 2019;165(3):269–275 doi:10.1093/jb/mvy114

JB THE JOURNAL OF BIOCHEMISTRY

Identification and biochemical characterization of a second zebrafish autotaxin gene

Received October 2, 2018; accepted December 18, 2018; published online January 10, 2019

Ryoji Kise[1], Ryohei Okasato[1], Kuniyuki Kano[1,2], Asuka Inoue[1,2], Atsuo Kawahara[3] and Junken Aoki[1,2,*]

[1]Graduate School of Pharmaceutical Sciences, Tohoku University, 6-3 Aoba, Aramaki, Aoba-ku, Sendai 980-8578, Japan; [2]AMED-LEAP, Japan Agency for Medical Research and Development, 1-7-1 Otemachi, Tokyo 100-0004, Japan and [3]Graduate School of Medical Science, Center for Medical Education and Sciences, University of Yamanashi, Shimokato 1110, Chuo, Yamanashi 409-3898, Japan

*Junken Aoki, Graduate School of Pharmaceutical Sciences, Tohoku University, 6-3 Aoba, Aramaki, Aoba-ku, Sendai, Miyagi 980-8578, Japan. Tel: +81-22-795-6860, Fax: +81-22-795-6859, email: jaoki@m.tohoku.ac.jp

Autotaxin (ATX) is a secreted enzyme that produces a bioactive lysophospholipid, lysophosphatidic acid (LPA). ATX plays a role in vascular and neural development in embryos but its mechanisms remain unclear. At the beginning of this study, only one zebrafish *atx* gene (*atxa*) was known and had been investigated. In this study, we generated ATX knockout (KO) fish by TALEN targeting *atxa*. Unexpectedly, *atxa* KO fish showed neither vascular defects nor reduction of ATX activity, implying the existence of one or more other ATXs in the genome. By a BLAST search using ATXa protein fragments as a query, we found a genomic sequence that closely resembled *atxa* exons 13, 14 and 15. Consequently, we cloned a cDNA encoding a second zebrafish autotaxin (ATXb), and found that it was transcribed in various tissues. The *atxb* gene encoded a protein of 832 amino acids (compared to 850 amino acids in ATXa) with 60% amino acid identity to ATXa and clustered with ATXs from other species. A recombinant ATXb protein showed lysophospholipase D (lysoPLD) activities with substrate specificities similar to those of ATXa and mammalian ATXs. These results indicate that ATXb is a second zebrafish ATX, which possibly shares redundant roles with ATXa in embryonic development.

Keywords: autotaxin; lysophospholipid; lysophosphatidic acid; zebrafish.

Autotaxin (ATX) is a secreted lysophospholipase D (lysoPLD) that produces a bioactive lipid, lysophosphatidic acid (LPA) from lysophospholipids such as lysophosphatidylcholine (LPC). LPA produced by ATX, in turn, activates six G protein-coupled receptors (GPCRs, $LPA_{1–6}$) and exerts various biological functions, such as fibrosis, implantation and hair follicle formation (*1–3*). In addition, ATX and LPA receptors are widely expressed during development (*4*, *5*). ATX knockout (KO) mice showed defects in nervous and vascular systems and died at embryonic day 9.5–10.5 (*6–8*). However, rodents are not well suited for studies in development because of the difficulty of the observation and manipulation.

ATX–LPA receptor axis is well conserved among vertebrates including zebrafish (*9*, *10*). In zebrafish, studies using recombinant ATX and recombinant LPA receptors indicated that zebrafish ATX and most of zebrafish LPA receptors displayed biochemical activities (*10*). Zebrafish are well suited for developmental studies because of their small size, high cost efficiency, transparency of embryos and development outside of the mother (*11*, *12*). We and others have utilized zebrafish to dissect the role of ATX in development using morpholino (MO)-based knockdown approaches, which suggested that ATX–LPA signalling may have roles in vascular development, cartilage formation and oligodendrocyte differentiation (*10*, *13–15*). However, a recent study comparing the phenotypes of MO-induced gene knockdown fishes and gene mutants revealed the vulnerability of the MO-based tools to dissect the gene functions because of the off-target effects of MO (*16*). In this study, we thus tried to generate the *atx* zebrafish mutants. Accordingly, we unexpectedly identified a second gene for *atx*, *atxb*.

Results

Establishment of *atxa* mutant fish

By TALEN-mediated mutagenesis, we generated *atx* KO zebrafish. *atx* (*atxa*) was registered as a unique gene in the zebrafish genome assembly Zv9 and was biochemically characterized (*10*). Accordingly, we established a mutant line with a 6-base pair (Bp) deletion near the catalytic active site in exon 7 (Fig. 1A). Amplification of mutant cDNA by RT-PCR in combination with DNA sequence analyses revealed that only cDNA with 49-Bp deletion was obtained as mutant cDNA. Importantly no cDNA with a 6-Bp deletion was obtained. The sequence analysis also revealed that a 6-Bp deletion in the genome created a new splicing donor site and caused abnormal splicing in the middle of exon 7, which explained the loss of 49-Bp from the intact cDNA (Fig. 1B). Since abnormal splicing caused the loss of the catalytically important threonine residue and generated a premature stop codon (Fig. 1B and C), the *atxa* mutant seemed to lack enzymatic activity. Intercrosses of heterozygous mutants revealed that homozygous mutants were viable and developed normally (data not shown). Furthermore, embryonic vascular formation of the homozygous *atxa* mutants was apparently normal (Fig. 1D). Thus, unlike in the case of mice and *atxa*-

MO-injected zebrafish embryos, the *atxa* mutant fish did not show vascular defects.

Evidence for the existence of a second *atx* gene in *atxa* KO fish

Since ATX protein is abundantly present in mammalian plasma, we next examined the enzymatic activity of the plasma from the *atxa* mutant fish. In mammals, almost all plasma lysoPLD activity is attributed to ATX (*7*, *17*). Consistent with this, application of an ATX inhibitor, ONO-8540506, suppressed most of the lysoPLD activity in plasma from wild-type zebrafish (Fig. 2). In addition, recombinant zebrafish ATXa was sensitive to ONO-8540506 (Fig. 5B). However, the lysoPLD activity of plasma collected from the *atxa* homozygous mutant fish was almost equal to that of wild-type zebrafish plasma (Fig. 2). Furthermore, the ATX inhibitor also suppressed the lysoPLD activity in plasma from homozygous *atxa* mutant fish (Fig. 2), indicating the presence of an ATX-like molecule other than ATXa. Considering the genomes of other fish species, such as fugu and medaka, encode two *atx* genes (*9*), these results suggested that zebrafish had a second *atx* gene.

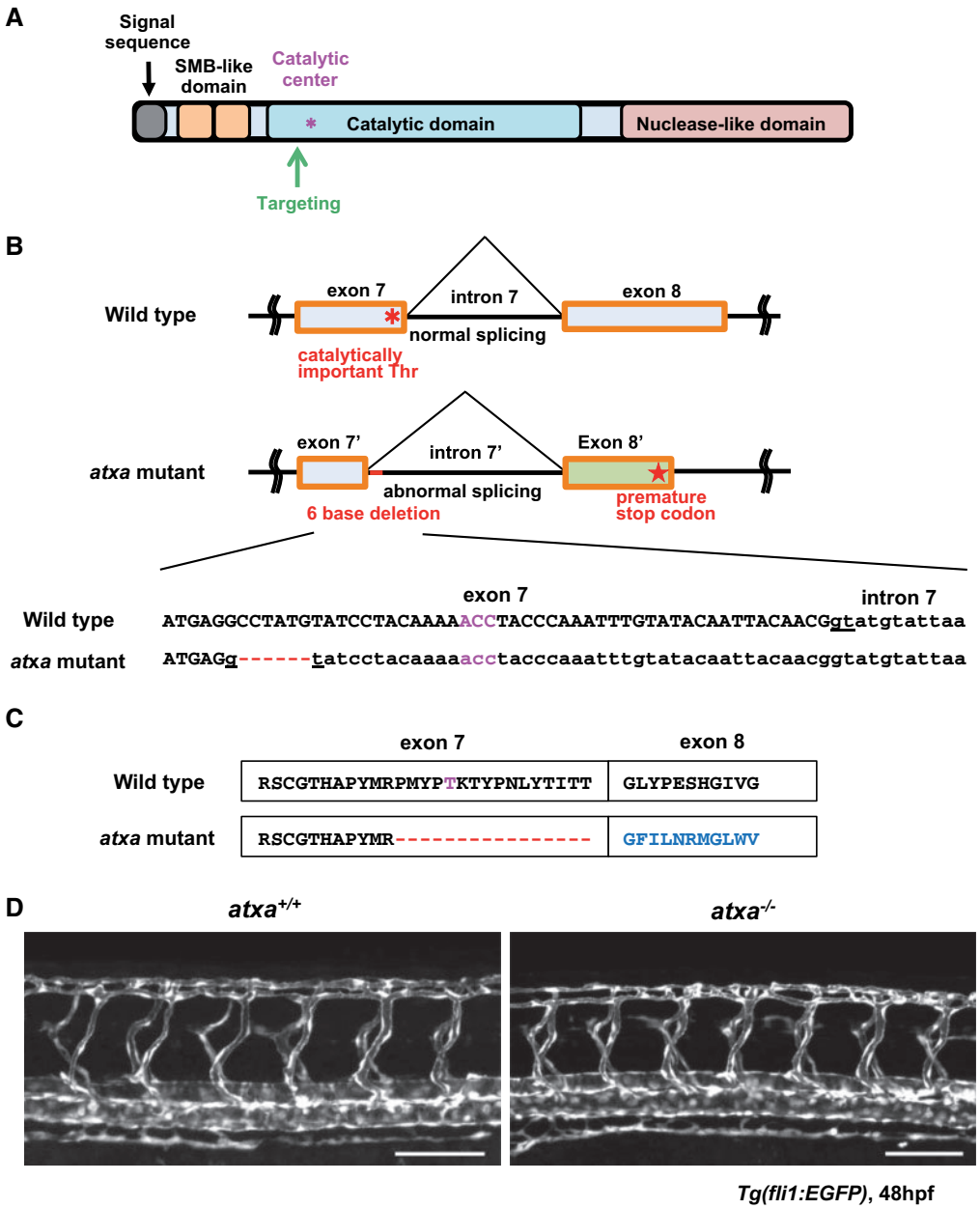

Fig. 1 Generation of *atxa* KO fish by TALEN-mediated mutagenesis. (**A**) Domain structure and targeting strategy for disruption of zebrafish *atxa*. For efficient gene disruption, nucleotides near the catalytic centre were targeted. SMB: somatomedin B-like. (**B**) Upper panel: Schematic drawing of exon–intron structure of zebrafish *atxa*. Line that indicates 6-bp deletion is highlighted. Catalytic centre is shown in asterisk. Stop codon is shown in star. Lower panel: The sequences of the exon–intron boundaries of zebrafish *atxa*. Upper and lower case letters indicate exons and introns, respectively. Splicing donor sites (gt) of wild-type and ATX mutant alleles are underlined. Nucleotides encoding catalytic amino acid are highlighted. (**C**) The protein sequences resulting from normal and aberrant splicing of exons 7 and 8. Catalytic centre of the enzyme is shown as magenta. (**D**) Confocal images of trunk vessels in 48 h post fertilization (hpf) *Tg(fli1:EGFP)* transgenic embryos. Scale bars: 100 μm.

Identification of a novel ATX-like gene fragment

To find the ATX-like gene, we searched the GRCz10 genome assembly using translated BLAST (tblastn).

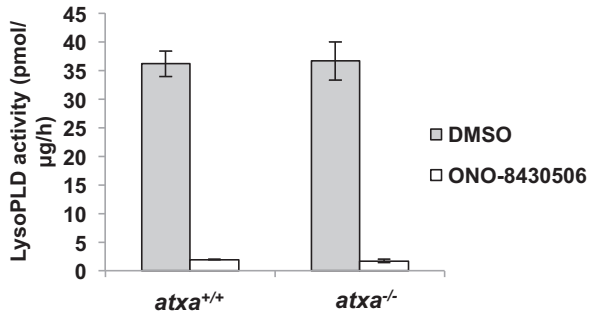

Fig. 2 Biochemical analysis of zebrafish plasma from *atxa* KO fish. LysoPLD activity of plasma from wild-type and homozygous *atxa* mutant zebrafish in the presence or absence of ATX inhibitor. Error bars indicate the SD of the mean ($n = 3$).

Amino acid sequences of each exon of ATXa were used as a query sequence. Consequently, we found a 452-Bp candidate sequence, which consisted of three exons (Fig. 3A). Each exon exhibited high sequence homology to exons 13, 14 and 15 of zebrafish *atxa* gene with 51, 64 and 79% identity at protein level, respectively (Fig. 3A and B). Since the corresponding sequence was not found in the expressed sequence tag (EST) database, we examined whether it was present in the zebrafish cDNA. By RT-PCR, the predicted cDNA sequence was correctly amplified using cDNA from various tissues tested, suggesting an ATX-like gene was actually transcribed and expressed in zebrafish tissues (Fig. 3C). Although the DNA sequences corresponding to exons other than exons 13–15 were missing in the database, multiple gap regions were found in the genome sequences upstream and downstream of the candidate sequence. We therefore hypothesized that the putative ATX-like genes have unassembled exons,

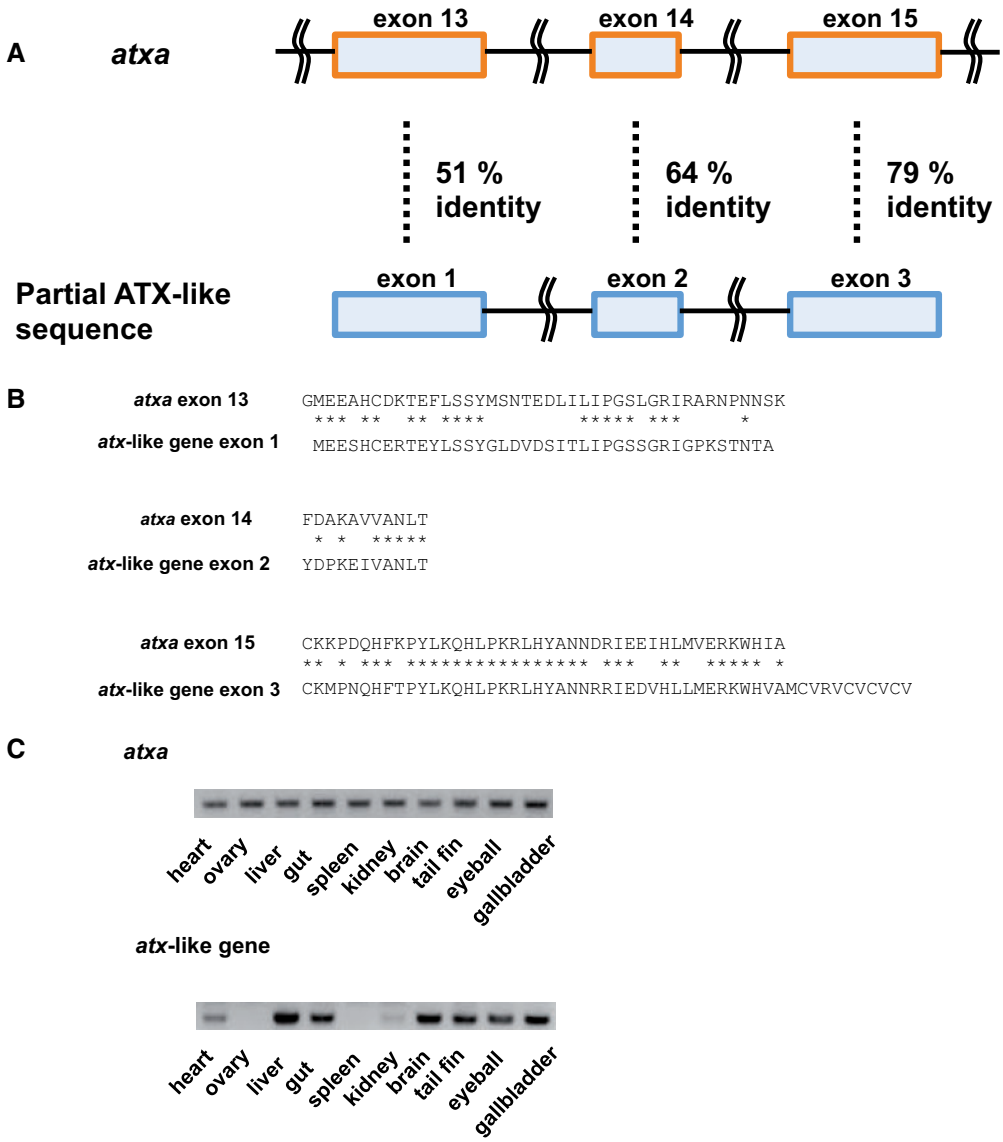

Fig. 3 Identification of a short *atx*-like sequence by BLAST homology search. (**A**) Comparison of protein sequence similarity between *atxa*- and *atx*-like gene. (**B**) Amino acid sequence comparison of *atxa*- and *atx*-like gene. Asterisks indicate identical amino acid residues. (**C**) RT-PCR analysis of gene expression of *atxa*- and *atx*-like gene in various zebrafish tissues.

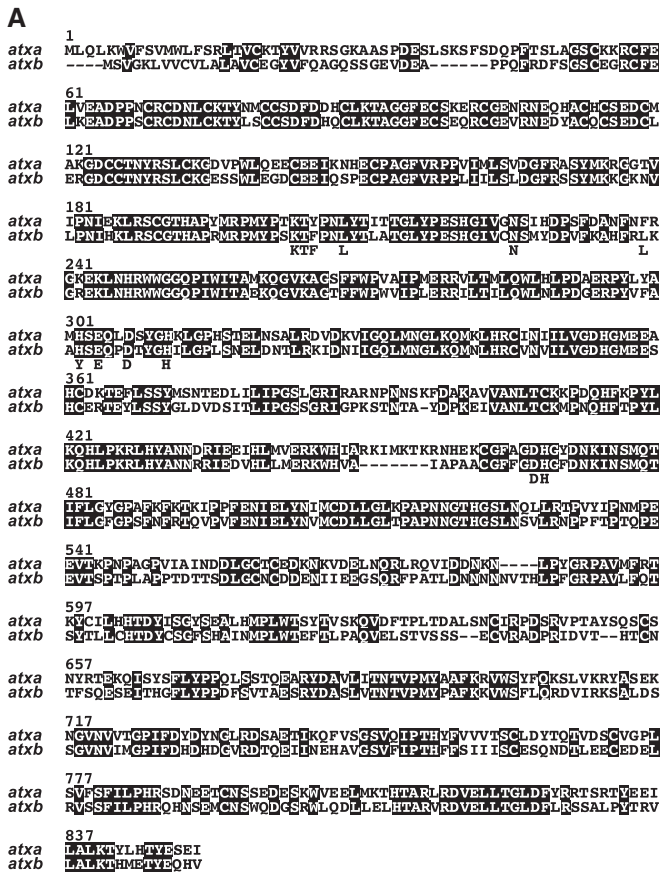

Fig. 4 Isolation of a novel zebrafish *atxb* gene. (**A**) Sequence alignment of zebrafish ATXa and ATXb. Residues conserved between ATXa and ATXb are highlighted with black. Residues involved in catalytic reaction and LPA recognition in mammals were indicated below zebrafish sequences. (**B**) Protein sequence conservation of ATX among vertebrates. zATX, zebrafish ATX; hATX, human ATX; mATX, mouse ATX; rATX, rat ATX. (**C**) Phylogenetic analysis of an identified gene against vertebrate ENPP family genes.

and decided to perform 5′- and 3′-RACE (Rapid Amplification of cDNA End) to isolate the full-length cDNA of the ATX-like gene.

Isolation of a second autotaxin gene in zebrafish

From the 452-Bp candidate sequence, we successfully amplified the 5′ and 3′ cDNA ends of an ATX-like gene by RACE. As a result, we obtained a cDNA encoding an ATX-like protein with a length of 832 amino acids (compared to 850 amino acids in ATXa), and with a 60% sequence identity to ATXa (Fig. 4A). Amino acids involved in the enzymatic reaction of ATX were largely conserved in the new gene (Fig. 4A). The new gene also showed moderate sequence identity to mammalian ATX (Fig. 4B) (*18*, *19*). ATX is a member of ectonucleotide pyrophosphatase/phosphodiesterase (ENPP) family, which comprises seven members (Enpp1-7). While ATX/ENPP2 hydrolyzes lysophospholipids, other members hydrolyze the pyrophosphate or phosphodiester bonds in nucleotide, glycerophosphocholine or sphingomyelin (*20*). Phylogenetic analysis demonstrated that the new gene clustered with other vertebrates ATXs among ENPP families (Fig. 4C). Thus, we assumed that the cDNA encoded a second ATX, and named it *atxb*.

Biochemical characterization of ATXb

To examine the enzymatic activity of ATXb, we overexpressed ATXb in HEK293 cells by transfecting them with the *atxb* cDNA and examined the lysoPLD

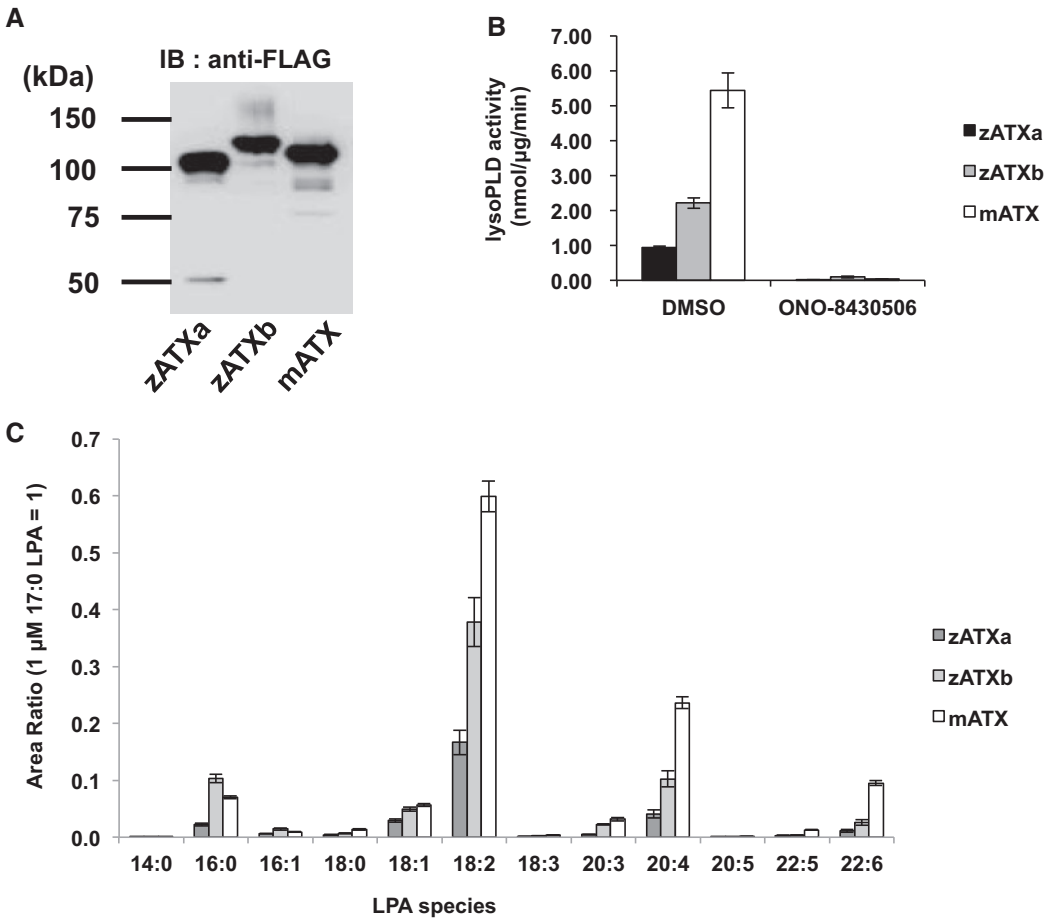

Fig. 5 Biochemical analysis of zebrafish ATXb. (**A**) Western blotting of culture supernatant of HEK293 cells transfected with a construct encoding FLAG-tagged mouse or zebrafish ATX. (**B**) LysoPLD activity of mouse and zebrafish ATX in the presence or absence of an ATX inhibitor. (**C**) LysoPLD activity of mouse and zebrafish ATX against physiological substrates. After incubation of recombinant ATX in mouse plasma, LPA production was evaluated by LC–MS/MS. Error bars indicate the SD of the mean.

activity in the cell supernatant. Like other ATX proteins, zebrafish ATXb was successfully recovered in the culture supernatant as judged by western blotting (Fig. 5A). The apparent molecular weight of zebrafish ATXb was higher than zebrafish ATXa possibly due to the difference of the extent of glycosylation. In an enzyme assay using an LPC as a substrate, ATXb showed significant lysoPLD activity, which was efficiently suppressed by an ATX inhibitor (Fig. 5B). We also examined the substrate specificity regarding the acyl chain of the ATX substrate. We used mouse plasma as a physiological substrate since it contains various types of LPC species. ATXb showed substrate specificities similar to those of mouse ATX and zebrafish ATXa (Fig. 5C).

Discussion

In this study, we identified a second zebrafish *atx* gene (*atxb*) that possessed enzymatic activity similar to ATXa. The finding that *atxa* homozygous mutant fish had ATX activity indicated that the zebrafish genome had another *atx* gene, which at the time of our study was not in the genome database (GRCz10). Because an ancestor of teleosts underwent an additional round of whole-genome duplication called the teleost genome duplication, a number of genes are duplicated in zebrafish. Partly because of its genome complexity, the zebrafish genome has many unsolved issues (https://www.ncbi.nlm.nih.gov/grc/zebrafish/issues). In the case of *atxb*, some gap sequences were found around a genomic region homologous to *atxa*, which prevented with the correct gene annotation. The newly released zebrafish database (GRCz11) has a cDNA sequence that completely matches the coding sequence of *atxb*, although it lacks accurate genomic information such as exon–intron junctions.

While embryos injected with *atxa*-targeting MO exhibited aberrant vascular formation, established *atxa* mutant fish did not show a similar vascular phenotype. The possible reasons for this contradictory result were discussed as follows: first, maternally derived mRNA rescued the early embryonic phenotypes of the *atxa* homozygous mutant. Second, vascular abnormalities observed in MO-injected embryos were caused by an off-target effect of MO and *atxa* did not contribute to vascular development. Third, *atxa*-targeting MO also suppressed *atxb* and the simultaneous knockdown of both *atx* genes caused vascular abnormalities.

However, the third explanation seems unlikely because the intron sequence targeted by MO is thought to be poorly conserved between *atxa* and *atxb*. To better understand the role of atx in vascular development, future studies of *atxa*/*atxb* double KO fish are needed.

Materials and Methods

Zebrafish

AB background transgenic fish, *Tg*(*fli1:EGFP*)^{y1}, was obtained from the Zebrafish International Resource Center (University of Oregon, Eugene, OR). Fish were maintained at 27–28°C under a controlled 13.5-h light/10.5-h dark cycle.

Reagent

ATX inhibitor, ONO-8430506 was kindly provided from Ono Pharmaceutical Co., Ltd.

ONO-8430506 was dissolved in DMSO and used at 10 μM.

Generation of *atxa* mutant fish by TALEN

TALEN construct targeting *atxa* was designed using online software (TAL Effector Nucleotide Targeter version 2.0, https://tale-nt.cac.cornell.edu). The left and right arms of TALEN targeting sequences were 5′-GTGGAACACATGCACCATACA-3′ and 5′-CCTACAAAAACCTACCCAA-3′, respectively. A targeting construct was generated by Golden Gate assembly method as previously described in (*21*). pRCIscript-GoldyTALEN was used as destination vector (*22*). The plasmid kit used for generation of TALENs was a gift from Daniel Voytas and Adam Bogdanove (Addgene kit # 1000000024). RCIscript-GoldyTALEN was a gift from Daniel Carlson & Stephen Ekker (Addgene plasmid # 38142). Vector was linearized by SacI digestion and mRNA was synthesized using mMESSAGE mMACHINE T3 kit (Ambion) and purified with the lithium chloride precipitation. Forward- and reverse-TALEN mRNAs (400 pg each) were injected together into one-cell stage embryos.

RT-PCR (Reverse transcription polymerase chain reaction)

Dissection of zebrafish organs was performed as previously described in (*23*). The total RNA was extracted by GenElute Total RNA Purification Kit (Sigma). Total RNA samples were reverse-transcribed using High-Capacity cDNA RT Kits (Applied Biosystems) according to the manufacturer's instructions. Polymerase chain reaction (PCR) was performed using primers listed in Supplementary Table S1.

LysoPLD assay

LysoPLD assay and preparation of recombinant ATX were performed as previously described with a minor modification (*10*). Zebrafish plasma was mixed with 2 mM 1-myristoyl-lysophosphatidylcholine and incubated at 37°C for 24 h. The amount of released choline was determined by colorimetrical assay. Zebrafish blood was collected as previously described in (*24*). Briefly, adult zebrafish was anaesthetized by ice-cold water and cut between the anal fin and the caudal fin with a surgical razor blade. Exuded blood was collected to the tube containing 5U/ml heparin and phosphate buffered saline (PBS). Collected blood was centrifuged at 500 *g*, 10 min and supernatant was used as plasma. Protein concentration was determined by bicinchoninic acid (BCA) assay (Thermo Fisher Scientific). The catalytic activity of zebrafish ATX against physiological substrates was determined as previously described in (*18*).

Confocal microscopy

Embryos were embedded in a drop of 1% low melting point agarose containing 0.01% Tricaine and 0.003% 1-phenyl-2-thiourea. Images were captured with a LSM 800 confocal laser-scanning microscope (Carl Zeiss) equipped with 10×/0.45 Plan-Apochromat.

Molecular cloning of the zebrafish *atxb*

Rapid amplification of 5′ and 3′ cDNA ends (RACE) was performed using a SMARTer RACE 5′/3′ kit (Takara Bio). 5′ cDNA fragment and 3′ cDNA fragment were obtained from total RNA isolated from zebrafish brain and tail fin, respectively. Primers used in RACE reactions were listed in Supplementary Table S1. The full-length zebrafish *atxb* was amplified by nested PCR and cloned into pCAGGS vector or pCAGGS-FLAG using NEBuilder HiFi DNA Assembly (NEBuilder HiFi DNA Assembly Master Mix, New England Biolabs). Amino acid sequences were aligned using ClustalW and viewed using JalView. A phylogenetic tree was constructed using ClustalW and visualized in FigTree software version 1.4.2.

Western blotting

Protein samples were separated by SDS–PAGE and transferred to nitrocellulose membranes using the Bio-Rad protein transfer system. The membranes were blocked with Tris-buffered saline containing 5% skimmed milk and 0.05% Tween 20, incubated with mouse anti-FLAG antibody (1E6, WAKO), and then treated with sheep anti-mouse IgG-horseradish peroxidase (GE Healthcare, NA931). Proteins bound to the antibody were visualized with an enhanced chemiluminescence kit (Amersham Biosciences).

Mass spectrometry

To examine the substrate specificities against physiological substrate, recombinant protein was added to pooled ICR mouse plasma and incubated at 37°C for 1 h, and then lipids were analysed. Production of various LPA species during the incubation was determined by LC–MS/MS as previously described in (*18*).

Supplementary Data

Supplementary Data are available at *JB* Online.

Funding

This work was supported by the Leading Advanced Projects for medical innovation (LEAP) (JP18gm0010004h0002 (to J.A.)) from the Japan Agency for Medical Research and Development (AMED) and KAKENHI (JP15H05899 (to J.A.)).

Conflict of Interest

None declared.

References

1. Kihara, Y., Mizuno, H., and Chun, J. (2015) Lysophospholipid receptors in drug discovery. *Exp. Cell Res.* **333**, 171–177
2. Yung, Y.C., Stoddard, N.C., and Chun, J. (2014) LPA receptor signaling: pharmacology, physiology, and pathophysiology. *J. Lipid Res.* **55**, 1192–1214
3. Aikawa, S., Hashimoto, T., Kano, K., and Aoki, J. (2015) Lysophosphatidic acid as a lipid mediator with multiple biological actions. *J. Biochem.* **157**, 81–89
4. Ohuchi, H., Hayashibara, Y., Matsuda, H., Onoi, M., Mitsumori, M., Tanaka, M., Aoki, J., Arai, H., and Noji, S. (2007) Diversified expression patterns of autotaxin, a gene for phospholipid-generating enzyme during mouse and chicken development. *Dev. Dyn.* **236**, 1134–1143
5. Ohuchi, H., Hamada, A., Matsuda, H., Takagi, A., Tanaka, M., Aoki, J., Arai, H., and Noji, S. (2008) Expression patterns of the lysophospholipid receptor genes during mouse early development. *Dev. Dyn.* **237**, 3280–3294
6. Koike, S., Yutoh, Y., Keino-Masu, K., Noji, S., Masu, M., and Ohuchi, H. (2011) Autotaxin is required for the cranial neural tube closure and establishment of the midbrain-hindbrain boundary during mouse development. *Dev. Dyn.* **240**, 413–421
7. Tanaka, M., Okudaira, S., Kishi, Y., Ohkawa, R., Iseki, S., Ota, M., Noji, S., Yatomi, Y., Aoki, J., and Arai, H. (2006) Autotaxin stabilizes blood vessels and is required

for embryonic vasculature by producing lysophosphatidic acid. *J. Biol. Chem.* **281**, 25822–25830

8. van Meeteren, L.A., Ruurs, P., Stortelers, C., Bouwman, P., van Rooijen, M.A., Pradere, J.P., Pettit, T.R., Wakelam, M.J., Saulnier-Blache, J.S., Mummery, C.L., Moolenaar, W.H., and Jonkers, J. (2006) Autotaxin, a secreted lysophospholipase D, is essential for blood vessel formation during development. *Mol. Cell. Biol.* **26**, 5015–5022
9. Fukushima, N., Ishii, S., Tsujiuchi, T., Kagawa, N., and Katoh, K. (2015) Comparative analyses of lysophosphatidic acid receptor-mediated signaling. *Cell. Mol. Life Sci.* **72**, 2377–2394
10. Yukiura, H., Hama, K., Nakanaga, K., Tanaka, M., Asaoka, Y., Okudaira, S., Arima, N., Inoue, A., Hashimoto, T., Arai, H., Kawahara, A., Nishina, H., and Aoki, J. (2011) Autotaxin regulates vascular development via multiple lysophosphatidic acid (LPA) receptors in zebrafish. *J. Biol. Chem.* **286**, 43972–43983
11. Lawson, N.D. and Wolfe, S.A. (2011) Forward and reverse genetic approaches for the analysis of vertebrate development in the zebrafish. *Dev. Cell* **21**, 48–64
12. Hogan, B.M. and Schulte-Merker, S. (2017) How to plumb a Pisces: understanding vascular development and disease using zebrafish embryos. *Dev. Cell* **42**, 567–583
13. Yuelling, L.W., Waggener, C.T., Afshari, F.S., Lister, J.A., and Fuss, B. (2012) Autotaxin/ENPP2 regulates oligodendrocyte differentiation in vivo in the developing zebrafish hindbrain. *Glia* **60**, 1605–1618
14. Lee, S.J., Chan, T.H., Chen, T.C., Liao, B.K., Hwang, P.P., and Lee, H. (2008) LPA1 is essential for lymphatic vessel development in zebrafish. *FASEB J.* **22**, 3706–3715
15. Nishioka, T., Arima, N., Kano, K., Hama, K., Itai, E., Yukiura, H., Kise, R., Inoue, A., Kim, S.-H., Solnica-Krezel, L., Moolenaar, W.H., Chun, J., and Aoki, J. (2016) ATX–LPA1 axis contributes to proliferation of chondrocytes by regulating fibronectin assembly leading to proper cartilage formation. *Sci. Rep.* **6**, 23433
16. Kok, F.O., Shin, M., Ni, C.W., Gupta, A., Grosse, A.S., van Impel, A., Kirchmaier, B.C., Peterson-Maduro, J., Kourkoulis, G., Male, I., DeSantis, D.F., Sheppard-Tindell, S., Ebarasi, L., Betsholtz, C., Schulte-Merker, S., Wolfe, S.A., and Lawson, N.D. (2015) Reverse genetic screening reveals poor correlation between morpholino-induced and mutant phenotypes in zebrafish. *Dev. Cell* **32**, 97–108
17. Saga, H., Ohhata, A., Hayashi, A., Katoh, M., Maeda, T., Mizuno, H., Takada, Y., Komichi, Y., Ota, H., Matsumura, N., Shibaya, M., Sugiyama, T., Nakade, S., and Kishikawa, K. (2014) A novel highly potent autotaxin/ENPP2 inhibitor produces prolonged decreases in plasma lysophosphatidic acid formation in vivo and regulates urethral tension. *PLoS One* **9**, e93230
18. Nishimasu, H., Okudaira, S., Hama, K., Mihara, E., Dohmae, N., Inoue, A., Ishitani, R., Takagi, J., Aoki, J., and Nureki, O. (2011) Crystal structure of autotaxin and insight into GPCR activation by lipid mediators. *Nat. Struct. Mol. Biol.* **18**, 205–212
19. Hausmann, J., Kamtekar, S., Christodoulou, E., Day, J.E., Wu, T., Fulkerson, Z., Albers, H.M.H.G., van Meeteren, L.A., Houben, A.J.S., van Zeijl, L., Jansen, S., Andries, M., Hall, T., Pegg, L.E., Benson, T.E., Kasiem, M., Harlos, K., Kooi, C.W.V., Smyth, S.S., Ovaa, H., Bollen, M., Morris, A.J., Moolenaar, W.H., and Perrakis, A. (2011) Structural basis of substrate discrimination and integrin binding by autotaxin. *Nat. Struct. Mol. Biol.* **18**, 198–204
20. Nakanaga, K., Hama, K., and Aoki, J. (2010) Autotaxin—an LPA producing enzyme with diverse functions. *J. Biochem.* **148**, 13–24
21. Cermak, T., Doyle, E.L., Christian, M., Wang, L., Zhang, Y., Schmidt, C., Baller, J.A., Somia, N.V., Bogdanove, A.J., and Voytas, D.F. (2011) Efficient design and assembly of custom TALEN and other TAL effector-based constructs for DNA targeting. *Nucleic Acids Res.* **39**, e82
22. Carlson, D.F., Tan, W., Lillico, S.G., Stverakova, D., Proudfoot, C., Christian, M., Voytas, D.F., Long, C.R., Whitelaw, C.B., and Fahrenkrug, S.C. (2012) Efficient TALEN-mediated gene knockout in livestock. *Proc. Natl. Acad. Sci. USA* **109**, 17382–17387
23. Gupta, T. and Mullins, M.C. (2010) Dissection of organs from the adult zebrafish. *J. Vis. Exp.* **37**, e1717
24. Pedroso, G.L., Hammes, T.O., Escobar, T.D., Fracasso, L.B., Forgiarini, L.F., and da Silveira, T.R. (2012) Blood collection for biochemical analysis in adult zebrafish. *J. Vis. Exp.* **63**, e3865